RSC Advances

PAPER

View Article Online
View Journal | View Issue

Cite this: *RSC Adv.*, 2024, **14**, 6856

Cesium tungsten oxide–carbon nanotube–hydroxypropyl cellulose thermoresponsive display

Taekyung Lim, Sang-Mi Jeong, Gun Hee Kim, Keumyoung Seo, Hee Sung Seo, Jonguk Yang* and Sanghyun Ju*

Among different heat-responsive polymers, hydroxypropyl cellulose (HPC) is biodegradable and is widely used in products that are harmless to the human body, such as food and pharmaceuticals. When the temperature of the hydrogel-type HPC increases, the hydrophilic bonds between the HPC molecules break, and the HPC molecules aggregate owing to the hydrophobic bonds. Therefore, light transmittance may vary because the aggregated HPC molecules scatter light. This study investigated the implementation of a display using the thermoreversible phase transition of HPC. Herein, a near-infrared (NIR) laser was irradiated only to a local area to control the surface temperature and enable the effective operation of the thermoreversible phase transition of HPC. For this, cesium tungsten oxide (CTO), which absorbs NIR light and generates heat, was mixed with the HPC hydrogel to improve the photothermal effect. Moreover, by additionally mixing carbon nanotubes (CNTs) with high thermal conductivity, the heat generated from the CTO is quickly transferred to the HPC hydrogel, and the heat of the HPC hydrogel is quickly cooled through the CNTs after stopping the NIR laser irradiation. The produced NIR-writing CTO–CNT–HPC (CCH) thermoresponsive display exhibited a fast thermoresponsive time. The CCH thermoresponsive display developed in this study can be applied in situations that require fast display response times, such as interactive advertising, property exhibitions, navigation systems for car, schedule information, event information, and public announcements.

Received 8th December 2023
Accepted 19th February 2024

DOI: 10.1039/d3ra08377b

rsc.li/rsc-advances

Introduction

Heat-sensitive polymers have amphiphilic polymer chains and exhibit a unique phase transition owing to the changes in their solvent interactions above a specific temperature. Heat-responsive polymers are classified into two categories depending on whether they exhibit a low critical solution temperature (LCST) or an upper critical solution temperature (UCST). Those exhibiting LCST interact well with solvents at temperatures below the LCST; however, at temperatures above the LCST, the interaction with solvents decreases as the coil-to-globule transition progresses.[1,2] Heat-responsive polymers exhibiting UCST are insoluble in solvents below the USCT but soluble at temperatures above the USCT.[3–5] Consequently, the polymer behavior according to the temperature induces a change in the hydrophilic–hydrophobic characteristics, varying the solubility in the solvent. These unique properties can aid in the design of innovative materials that respond only to specific temperatures. Heat-responsive polymers have been studied for applications in various industries, such as drug delivery systems, actuators, and filters.[6–9] Among different heat-responsive polymers, hydroxypropyl cellulose (HPC), which exhibits LCST behavior, is biodegradable. It is widely used in products that are harmless to the human body, such as food and pharmaceuticals,[10,11] because it is an eco-friendly material.[12]

Precise temperature control is required to effectively control the changes in the hydrophilic–hydrophobic properties of heat-sensitive polymers. Cesium tungsten oxide (CTO) is widely known as a photothermal material that absorbs a near-infrared (NIR) wavelengths and immediately converts them into thermal energy. For CTO doped with cesium in tungsten oxide, the near-infrared (NIR) absorbance increases with cesium doping.[13,14] Photothermal materials, such as CTO, are primarily applied to the biomedical field of photothermal therapy (PTT) and are used to remove tumors such as cancer cells.[15,16] carbon nanotubes (CNTs) have high thermal conductivity, facilitating the transfer of thermal energy, thermal diffusion, and cooling. It is an accessible heat-dissipation material. Multi-walled CNT (MWCNT) has a high thermal conductivity of ~3000 W m^{-1} K^{-1},[17] and the thermal conductivity of polydimethylsiloxane (PDMS) mixed with 10 wt% of CNT is ~0.45 W m^{-1} K^{-1}. In a previous study, this was improved by ~2.4 times compared to pristine PDMS, having a density of 0.1884 W m^{-1}·k.[18]

This study converted the hydrophilic–hydrophobic properties of HPC through precise temperature control by irradiating a local area using an NIR laser. The coil (hydrophilic)-to-global

Major in Nano·Semiconductor, School of Electronic Engineering, Kyonggi University, Suwon, Gyeonggi-do 16227, Republic of Korea. E-mail: juyang@kgu.ac.kr; shju@kgu.ac.kr

(hydrophobic) transition of the HPC hydrogel according to the LCST visibly changed the light transmittance reversibly, and this was utilized to produce a display. To effectively induce a phase change in HPC and a corresponding change in the visible light transmittance by rapidly changing the temperature above or below the LCST, CTO with high NIR absorbance and CNT with high thermal conductivity were mixed in the HPC hydrogel at an optimal ratio. Generally, it is challenging to heat and cool thermal energy only in a local area. Even if rapid heating is possible, it is difficult to control the corresponding rapid cooling. The NIR-writing CTO–CNT–HPC (CCH) thermoresponsive display produced in this study induced a visible change in transmittance by irradiating with an NIR laser and increasing the temperature of only the relevant area above the LCST. In addition, display driving was achieved using the CTO and CNT to enable rapid heat absorption and cooling. This display can be easily fabricated by filling rigid glass and flexible polymer substrates with a CCH composite hydrogel for bending.

Experimental

Preparation of materials

The nano-CTO dispersion was prepared by dispersing CTO (V9, 20–40 nm, CFC tetramate) powder at 1 wt% in distilled (DI) water, followed by milling with a roller-type ball mill (M03-02-115, LKlab Korea) at 200 rpm. The dispersion preparation incurred 14 days. The CTO powder was pulverized using a 1 mm zirconia ball. CNTs (MWCNT–OH functionalized, 10–20 nm, SkySpring Nanomaterials) with hydroxyl groups substituted on the CNT surface were used, and UV/ozone (UVO Cleaner, AhTECH Leading Technology Systems Co.) was used to create more polarity. The HPC (Mw ~100 000, Sigma-Aldrich) hydrogel was mixed with the CTO–CNT solution without further purification.

Synthesis of CCH composite hydrogel

The UV/ozone-treated CNTs were mixed with 100 g of 1.0 wt% nano-CTO dispersion at 0.025–0.5 wt%. The CTO–CNT solution was sonicated for 15 min using an ultrasonicator (Q500, Qsonica) to obtain a uniform dispersion. HPC was added at 15 wt% to the CTO–CNT dispersion and mixed vigorously for 5 min using a vortex mixer (VM-10, DAIHAN Scientific).

NIR-writing CCH thermoresponsive display production and operation

Slide glass (0350-0001, 76 × 52 mm^2, LKlabKorea) was used as the flat substrate, and a polyethylene naphthalate (PEN) film (Teonex Q65HA, Teijin Dupont Films) was used as the curved substrate. After washing the flat and curved substrates with isopropyl alcohol (IPA) and DI water, they were treated with a UV/ozone cleaner for 10 min to obtain a superhydrophilic substrate. Subsequently, a double-coated tape (VHB, 0.5 T, 3M) was attached to three sides of the board, and another board was layered on top to create a space with only one side open. The prepared CCH composite hydrogel was slowly injected into the space between the two substrates using a syringe and 23G needle. The residual bubbles generated during hydrogel injection were removed under vacuum. Subsequently, the CCH thermoresponsive display was fabricated by completely sealing one open side with silicone (00-30, Ecoflex). To drive the CCH thermoresponsive display, various images were obtained using an NIR laser-marking machine (Mini1064-30, Changchun New Industries Optoelectronics Tech. Co., Ltd) at a wavelength of 1064 nm. The NIR laser application conditions (power, speed, and repetition) during the measurement process were 6 kW, 1300 mm s^{-1}, and 20 kHz, respectively. The NIR laser was scanned to the desired design using the EzCad2 software (ver. 2.9.9, Beijing JCZ Technology Co., Ltd). The distance between the NIR laser head and the CCH thermoresponsive display surface was approximately 190 mm. During NIR laser irradiation, an IR camera (T420, FLIR® Systems, Inc.) was used to check the heating temperature on the surface of the CCH thermoresponsive display. The luminance value of the image of the white figure shown when running the CCH thermoresponsive display was extracted and analyzed using an open-source-based tracker program (video analysis and modeling tool, **https://physlets.org/tracker/**).

Results and discussion

Fig. 1a shows the operating image of the NIR-writing CCH thermoresponsive display based on the laser application. The CCH thermoresponsive display operates by scanning an NIR laser on the CCH thermoresponsive display, formed by inserting a CCH composite hydrogel between two transparent substrates (glass or PEN film). The heat was generated by irradiating a specific area of the CCH composite hydrogel using an NIR laser, and the area changed from transparent to white owing to the resulting phase change of the HPC. The cellulose series in the hydrogel state underwent a phase change based on the LCST of 40–70 °C.[12,19–21] The HPC hydrogel matrix contains hydroxypropyl groups that have hydrophilic and hydrophobic properties. At temperatures below LCST, the hydrophilic O–H is well dispersed through the hydrogen bonding with water and appears as a transparent solution. When the temperature of the HPC rises above the LCST, a coil-to-globule transition occurs because of the strong interaction between the hydrophobic C–H within the hydroxypropyl groups, leading to the scattering of light and rendering the display visible.[22,23] In addition, dehydration occurs owing to interference with the hydrophilic O–H hydrogen bond, which can also be observed in the viscosity change of the HPC hydrogel matrix below and above the LCST temperature. The viscosity of HPC increases owing to hydrogen bonding with water at temperatures below the LCST. However, at temperatures above the LCST, the viscosity decreases to a level close to that of water through dehydration.[24] Therefore, HPC hydrogel remains dispersed in water at temperatures below the LCST. However, dehydration and aggregation occur when the temperature rises above the LCST, and HPC hydrogel becomes visible (Fig. 1b). CTO, tungsten oxide (WO_3) doped with cesium (Cs), absorbs the NIR wavelength band by forming a conduction band at a low level.[25–27] CTO absorbs electromagnetic waves at NIR wavelengths through a polaron mechanism.

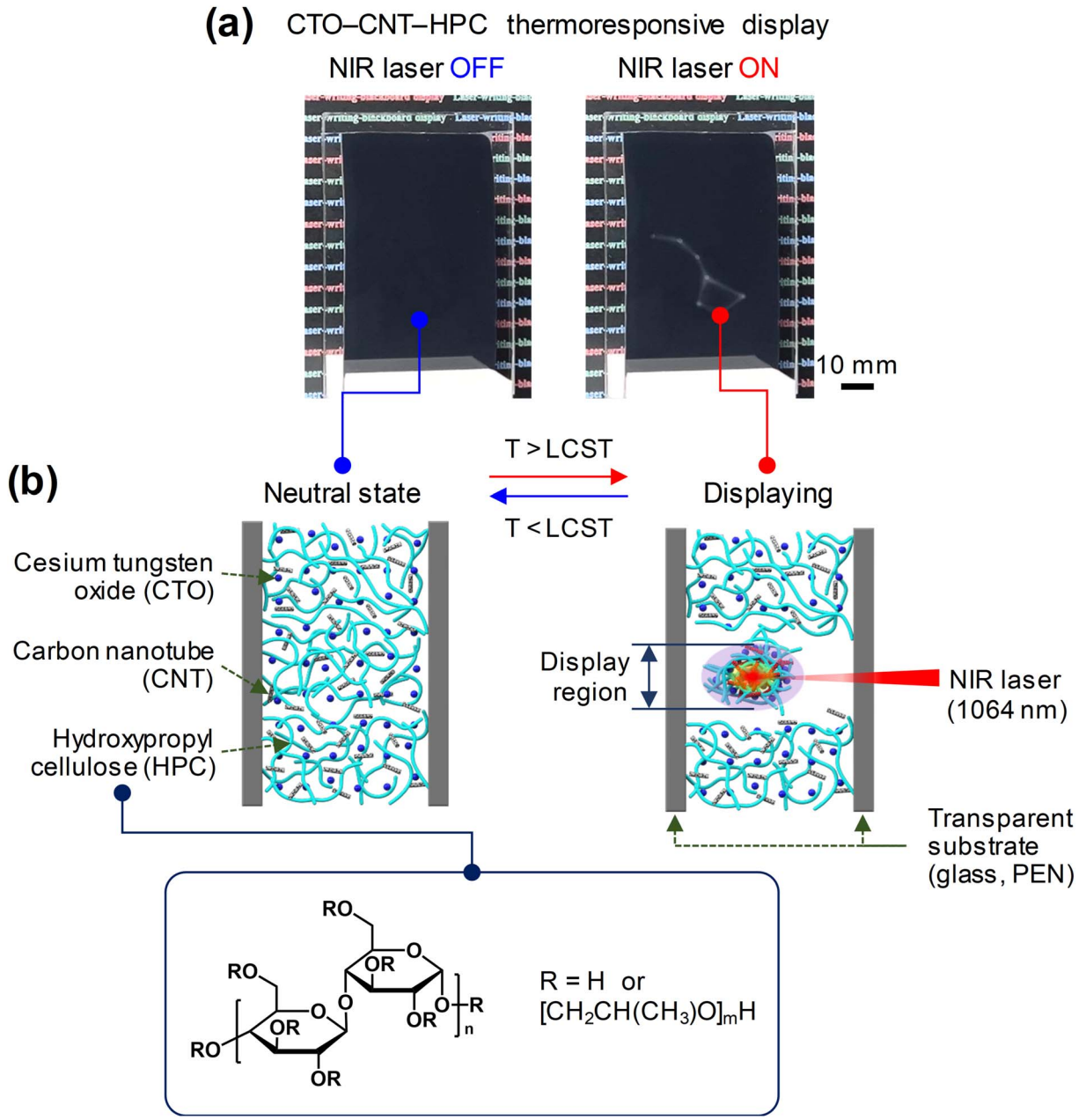

Fig. 1 Driving mechanism of NIR-writing CCH thermoresponsive display. (a) Color changes in the image with and without NIR laser irradiation on the surface of CCH composite hydrogel. (b) Schematic illustration of the structural changes inside the CCH composite hydrogel based on the application of NIR laser.

It absorbs energy[14,28] and dissipates it as heat.[29] In addition, the absorption spectrum of the CNTs shows that absorption occurred in the NIR region, and the absorbed energy was released as heat.[15,16] Therefore, when an NIR laser with a wavelength of 1064 nm is irradiated onto a CCH thermoresponsive display, the CTO and CNT simultaneously absorb the NIR laser and radiate heat energy. The radiated heat is transferred to the entangled HPC hydrogel matrix. When the temperature reaches the LCST, a coil-to-globule transition of the HPC is induced, resulting in a dehydration reaction. Thus, only the area irradiated by the NIR laser is visualized as white.

Fig. 2a shows the heating temperature of the CCH composite hydrogel depending on whether the NIR laser was applied. When the NIR laser on/off section was set to 30/30 s, the overall temperature continued to increase with irradiation time. At 30 s after the NIR laser was applied, the temperatures were 36.67, 38.72, 40.52, 41.10, and 42.03 °C (0, 0.025, 0.050, 0.075, and 0.100 wt%, respectively) depending on the CNT content. This shows that the material that absorbs wavelengths in the NIR region is CTO (or CWO; Cs_xWO_3) and is the photothermal effect of CNT. After 30 s, when the NIR laser was applied, the temperature decreased owing to thermal diffusion. It was

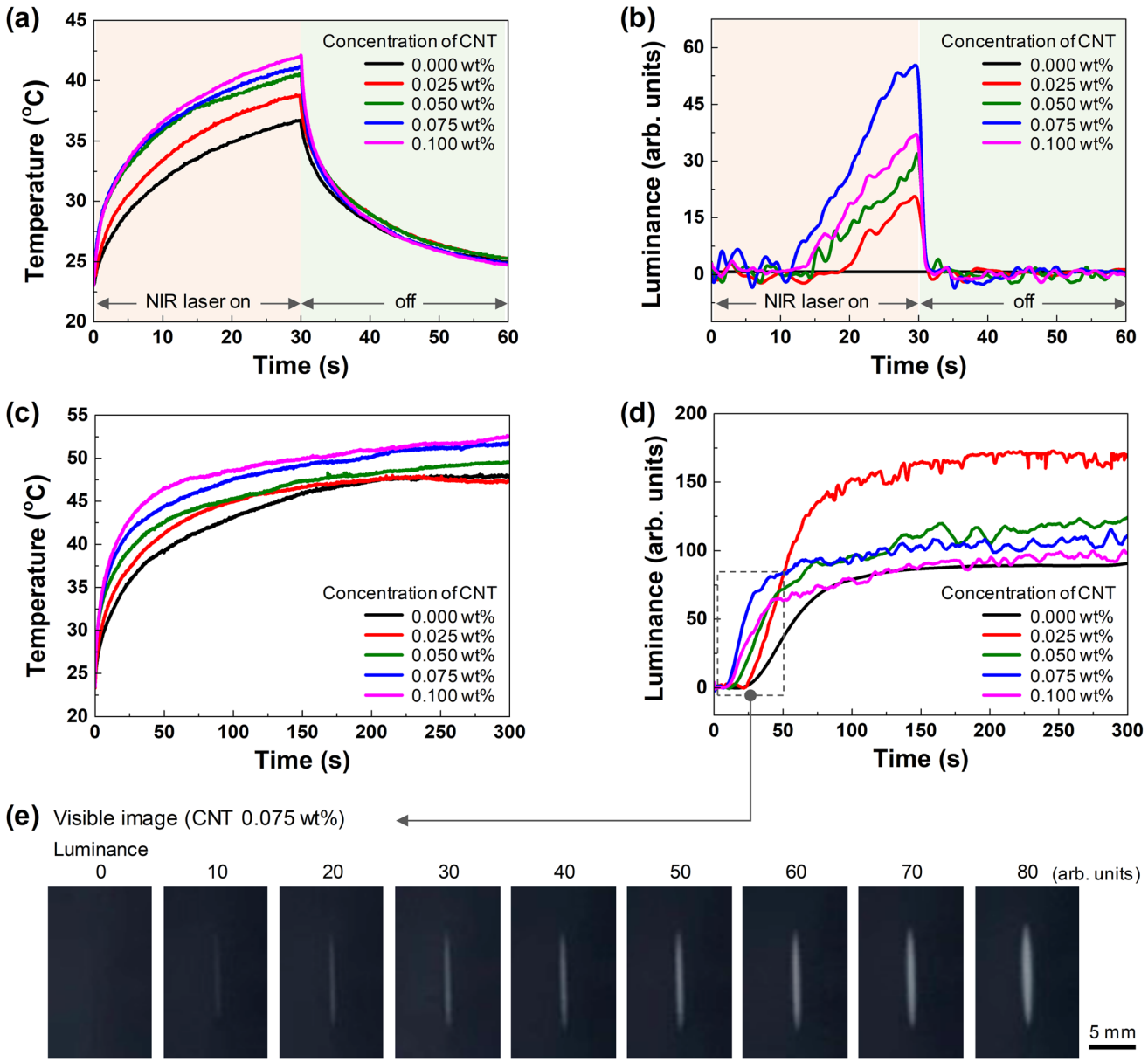

Fig. 2 Heat generation and visualization characteristics of CTO–HPC composite hydrogel by CNT content. Trends of (a) heating temperature and (b) luminance change according to NIR laser on/off (30/30 s) on the CCH thermoresponsive display with CCH composite hydrogel applied by a CNT content of 0–0.1 wt%. (c) Heating temperature and (d) luminance change trend according to the continuous application of the NIR laser and (e) actual image according to the luminance value at 0.075 wt% of CNT.

confirmed that the temperature dropped again to room temperature without any significant effect.

Fig. 2b shows the effect of turning the NIR laser on/off on the visible light change, depending on the CNT content. When an NIR laser was applied under the same conditions, no visible changes were observed at 0 wt%. However, a change occurred from 0.025 wt%. At the maximum temperature point of 30 s, the luminance values were 20.6, 31.54, 55.29, and 36.75 (0.025, 0.050, 0.075, and 0.100 wt%, respectively). The exothermic temperature increased with the CNT content, and the number of internally deformed molecules in the hydrogel increased with the temperature delivered to the HPC. Therefore, the luminance appeared to increase with temperature. However, as shown in Figure 2b, 0.075 wt% appeared to be higher than 0.100 wt%. This is because the luminance was calculated using the RGB values of the digital image. According to the numerical value in the formula, black has a luminance of zero, while white has a luminance of 250. This study measured the visible changes as the value increased from zero, using a white pattern in the CCH thermoresponsive display. However, as the CNT content increased, the irradiation area of the NIR laser changed to white. Nevertheless, the CNT (black color) was also entangled internally; hence, the luminance tended to decreased. In addition, the timing of the change in luminance varied depending

on the CNT content. As the temperature of the HPC rises faster, the time it takes to reach LCST becomes faster, resulting in a faster color change to white. The point at which the temperature changes rapidly for HPC to reach LCST is 18.9 s for 0.025 wt% CNT and 11.7 s for 0.075 wt% CNT. As the CNT content increases, the time to reach LCST becomes faster. This is the display response of the NIR laser, which is referred to as the response time. Note that 0.100 wt% CNT showed a slowing of discoloration owing to the influence of the CNT inside.

As shown in Fig. 2c, the NIR laser was continuously applied for 300 s without an off period, depending on the CNT content. A section was observed where the temperature increased over time and gradually slowed after 180 s. The luminance changed after 30 s at 0 wt% (Fig. 2d). This indicates that more than 30 s of application is required under the same NIR laser conditions. At 0.025 wt%, the luminance was relatively low before 30 s but showed the highest value after fully reaching the LCST. Furthermore, 0.075 wt% had a higher heating temperature than 0.025 wt%; therefore, the luminance change was fast, and the luminance value was low because of the color of the CNT. When the visible image was checked for different luminance values, the white color became increasingly evident in 10 units from 0 to 80 (Fig. 2e). The pattern size was a 10 mm line. The CCH composite hydrogel with a CNT content of 0.075 wt% exhibited the fastest response. Although the luminance value was not the highest, it was greater than 60, which could be distinguished visually, making it optimal. The minimum line width at 10, which is the minimum luminance value that can be confirmed with the naked eye, was 0.62 mm.

Fig. 3 shows the difference between the IR and visible images depending on the CNT content, 30 s after applying the NIR laser to the CCH composite hydrogel. When used for 30 s under the same conditions, the temperature of the center where the laser was applied increased depending on the CNT content, and the red color became more evident. A visible pattern caused by the HPC heat can be observed, and it was confirmed that the line width remained around 1.2 mm through visible images.

To confirm the effect of CNT on the CCH thermoresponsive display, CNT 0 wt% and CNT 0.075 wt% were compared. First, the temperature and luminance of the CCH composite hydrogel (CNT 0 wt%) were confirmed by repeated application of an NIR laser. In Fig. 4a, the on time is 5 s, and the off times are 5, 7, and 10 s. As the off time increased, the temperature at 300 s decreased. This shows that the NIR laser generates heat, and as the cooling time decreases, the heat inside the hydrogel accumulates. No change in luminance was observed owing to insufficient application of the NIR laser. When enlarged at the 26th time (~262 s) of 5/5 s, there was no change in luminance even though heat was generated up to 37.5 °C (Fig. 4d). At an on time of 7 s, the luminance value decreased as the off time became longer, from ~20 at off time 5 s, less than 20 at off time 7 s, and 0 at off time 10 s. No change appeared (Fig. 4b). This is a phenomenon in which the NIR laser application for 7 s is not enough to reach the LCST. However, if the off time is short, heat spreads internally and accumulates as the next NIR laser is applied before reaching room temperature. In Fig. 4e, during 24 times (~278 s) of on/off 7/5 s, the maximum temperature was 39.26 °C, and the maximum luminance was 19.5. The luminance below 20 was relatively faint, but a white pattern was formed (Fig. 2e). The point at which visible changes appear was delayed from the point of the NIR laser. The delay time was 2.8 s, and the fading time when the pattern disappeared from the NIR laser-off point was 2.6 s. At the fading time, the luminance changed from 19.5 to 2.9.

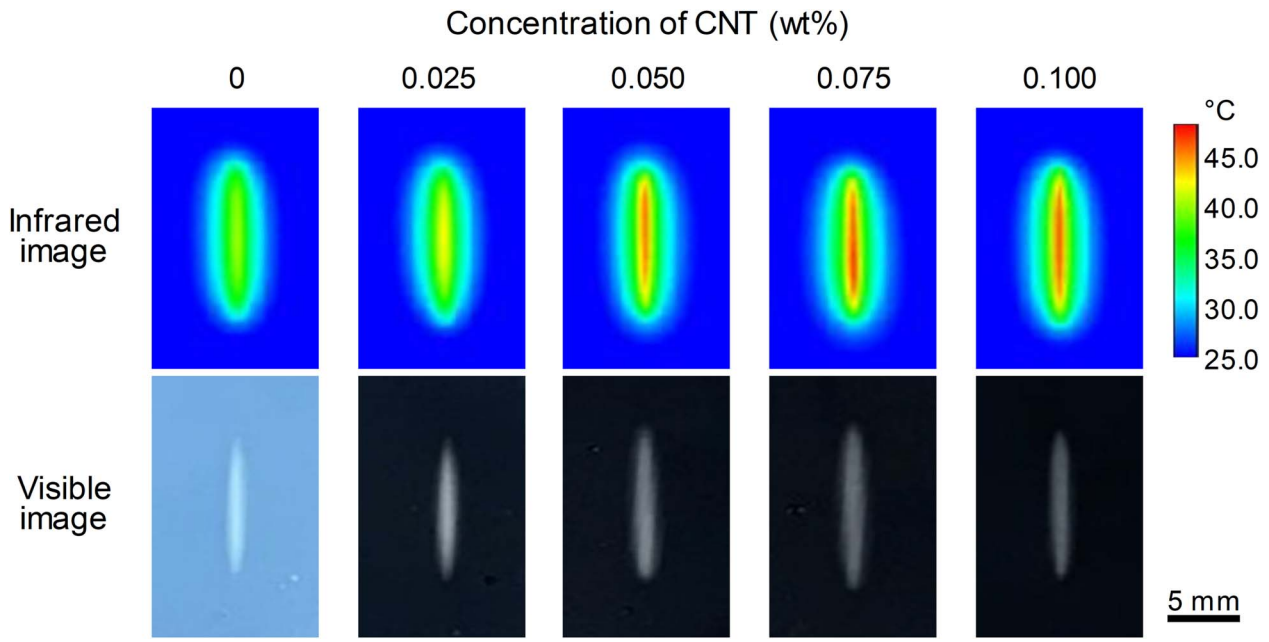

Fig. 3 Heat generation and visualization images of CTO–HPC composite hydrogel by CNT content. IR and visible images at 30 s when an NIR laser is applied to a CCH thermoresponsive display with CCH composite hydrogel of 0–0.1 wt% CNT content.

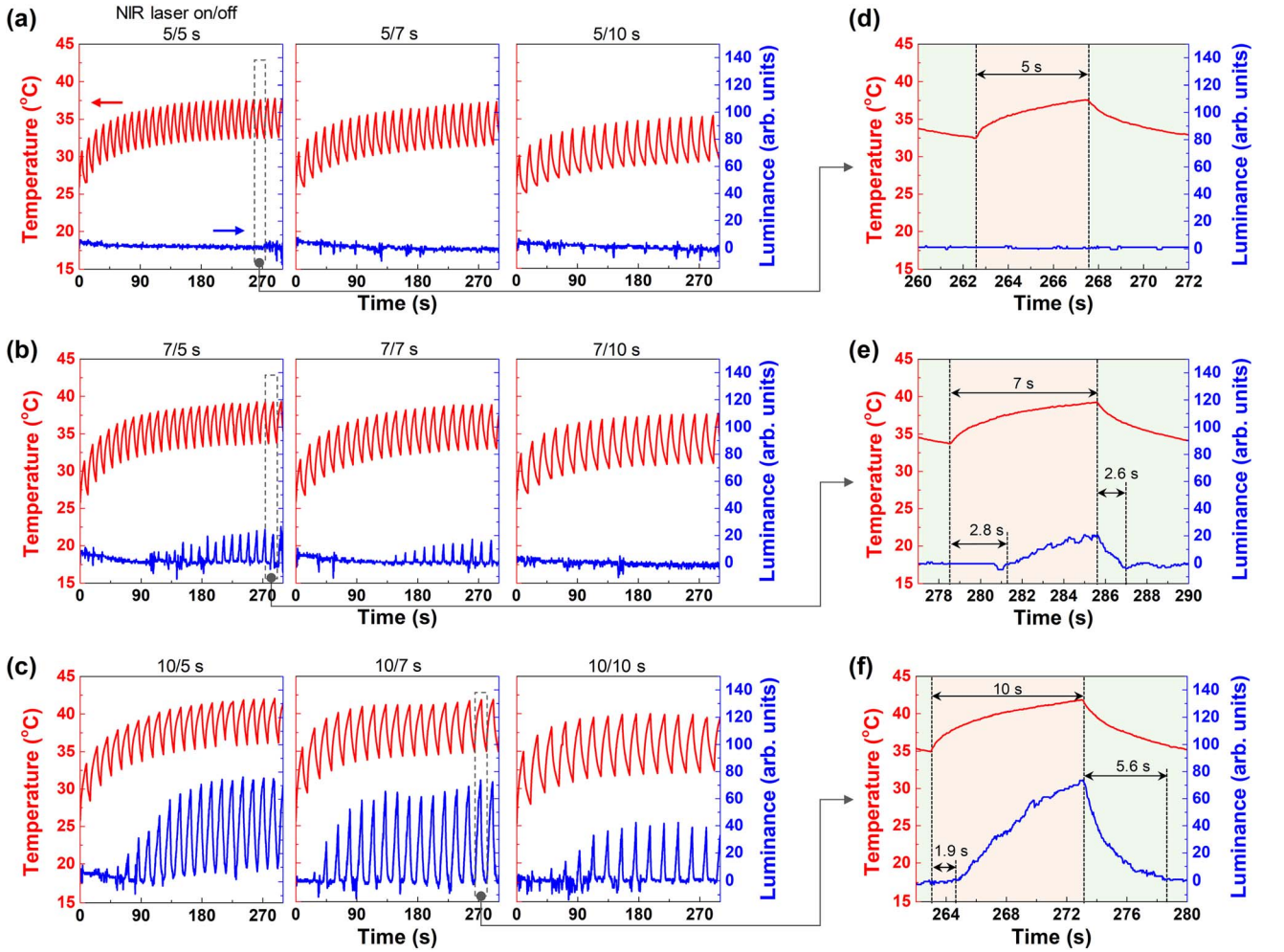

Fig. 4 Repetitive display characteristics of CCH composite hydrogel (CNT 0 wt%). Heat generation and luminance characteristics according to the periodic application of the NIR laser to the CCH composite hydrogel (CNT 0 wt%). NIR laser application on/off conditions—(a) 5/5, 7, and 10 s, (b) 7/5, 7, and 10 s, and (c) 10/5, 7, and 10 s. Heat generation and luminance response characteristics according to NIR laser application (NIR laser on/off representative conditions—(d) 5/5 s, (e) 7/5 s, and (f) 10/7 s).

Most of the white patterns appeared at an NIR laser-on time of 10 s. In Fig. 4c, at an on/off time of 10/5 s, cumulative heat exceeding 40 °C was generated, and the luminance changed rapidly. Changes in luminance, including noise, were observed for the second time. However, owing to insufficient off time, the bottom section of the luminance increased gradually. At 10/7 s, the luminance of the bottom section was maintained close to zero; therefore, it operated relatively stable. At 10/10 s, it can be observed that the bottom was maintained in the off time. During 16 times (~264 s) at 10/7 s, the maximum temperature was 41.84 °C, the delay time was 1.9 s, and the fading time was 5.6 s. At the fading time, the luminance decreased from 73.69 to 1.51 (Fig. 4f).

Fig. 5 shows the characteristics of the CCH composite hydrogel (CNT content = 0.075 wt%). Fig. 5a shows the attributes of the NIR laser by fixing the on time to 5 s and changing the off time to 5, 7, and 10 s. When the off time was 5 s, the luminance value appeared to be less than 20 in the first four repetitions. The luminance value was ~40 from the fifth repetition onward, displaying a white pattern. When the on time/off time was 5/5 s, the temperature of the HPC, which started at ~25 °C, was maintained in the lower range at ~35 °C even when the NIR laser was turned off. Comparing this to 10/5 s in Fig. 5c, where the on time of the NIR laser is longer than the off time, the lower temperature range due to heat accumulation increases to ~38 °C. At approximately 200 s, the luminance does not decrease completely.

This shows that the HPC molecules that underwent the coil-to-globule transition did not have enough time to recover in the section below the LCST. As the NIR laser is irradiated, the starting temperature of the following pattern progresses to a higher temperature than the initial temperature, showing that the lower section rises. Therefore, designing a pattern and setting conditions considering the correlation between the accumulated heat according to the on time of the NIR laser and the recovery time according to the off time was necessary. As shown in Fig. 5b, even at 7/5 s, the on time is longer than the off

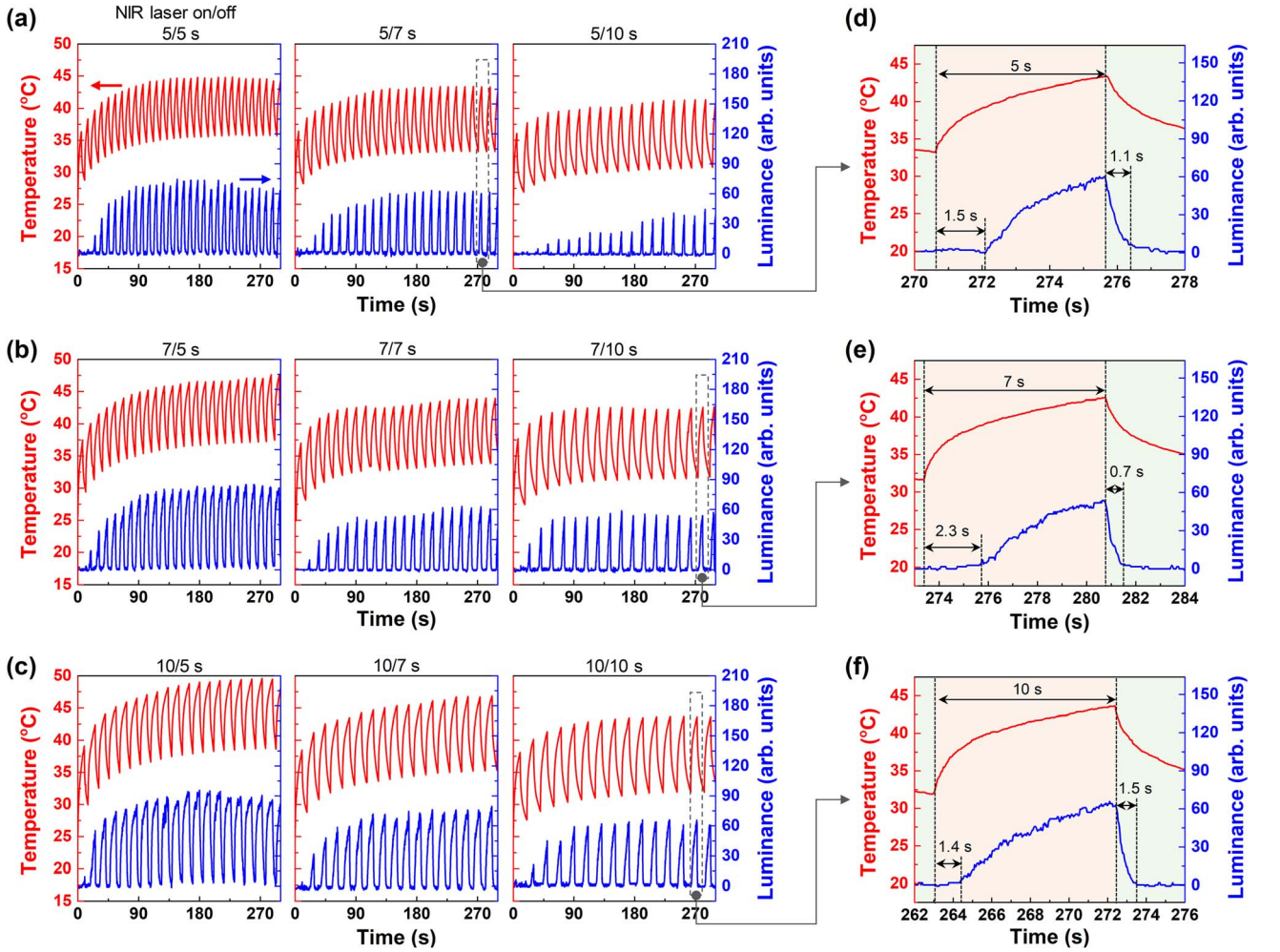

Fig. 5 Repetitive display characteristics of CCH thermoresponsive display (CNT 0.075 wt%). Heat generation and luminance characteristics according to periodic application of NIR laser to CCH composite hydrogel (CNT 0.075 wt%). NIR laser application on/off conditions—(a) 5/5, 7, and 10 s, (b) 7/5, 7, and 10 s, and (c) 10/5, 7, and 10 s. Heat generation and luminance response characteristics according to NIR laser application (NIR laser on/off representative conditions—(d) 5/7 s, (e) 7/10 s, and (f) 10/10 s).

time; therefore, the next NIR laser was applied with the bottom section of the luminance at off rising from 24 times (~280 s).

In Fig. 5d–f, the on/off response time is confirmed in the relatively stable section, where the luminance value is at the bottom in the off state. Fig. 5d shows an enlarged graph at repetition 23 when the on/off is 5/7 s. The temperature rose immediately after applying the NIR laser, but the luminance value increased after a 1.5 s delay. The luminance value at the point where it was turned on for 5 s was 59.93, and the fading time confirmed that the luminance decreased to 4.23 in 1.1 s after the NIR laser was turned off. At 7/10 s, as shown in Fig. 5e, the delay time was 2.3 s, the fading time was 0.7 s, and the luminance value decreased from 53.82 to 3.8. As shown in Fig. 5f, the delay time was 1.4 s, the fading time was 1.5 s, and the luminance decreased from 64.10 to 2. Overall, the delay time in changing to white occurred $\sim 1.7 \pm 0.4$, and the fading time for restoration was as short as $\sim 1.1 \pm 0.3$ s. In Fig. 4, for the CTO–CNT–HPC composite hydrogel with CNT 0 wt%, the delay and fading time were $\sim 2.4 \pm 0.5$ s and $\sim 4.1 \pm 1.5$ s, respectively. The CCH composite hydrogel (CNT 0.075 wt%) had a relatively short delay and fading time, even though the off time was extended. Hence, the CNTs contribute to NIR absorption and heat generation, helping in white pattern formation, and heat diffusion, thereby reducing the fading time.

Fig. 6 shows the operating images of a CCH thermoresponsive display with flat and curved shapes. A dual structure was produced by inserting a CCH composite hydrogel (CNT 0.075 wt%) between a glass or PEN film. Various geometric patterns were formed through the NIR laser irradiation of the fabricated CCH thermoresponsive display of size 76 × 52 mm^2. As shown in Fig. 6b and e, various white pattern images (hexagons, stars, hourglasses, and emoji) and text ('CNT') were formed on the flat and curved (curvature radius 38 mm) substrates. In addition, a constellation (Big Dipper) was formed point-by-point by sequentially displaying the changing images using an NIR laser. Ultimately, the changes connecting each point were implemented as a continuous image (Fig. 6c and f).

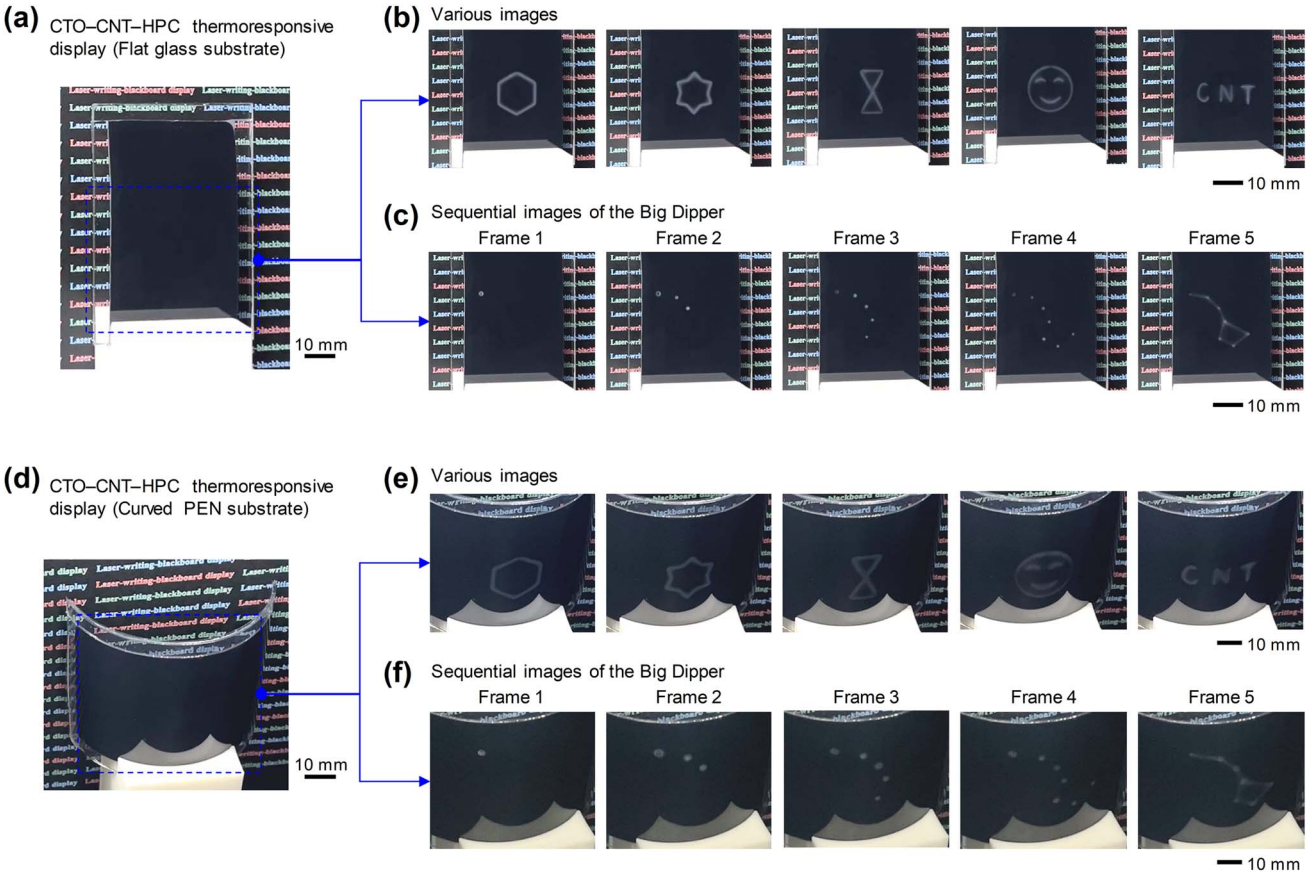

Fig. 6 CCH thermoresponsive display operation. Actual image of the display with CCH composite hydrogel (CNT 0.075 wt%) composed of (a) flat and (d) curved shapes. Sequential images of (b and e) various shapes and (c and f) constellations (Big Dipper) formed in white by the CCH thermoresponsive display.

Conclusion

This study fabricated a CCH composite hydrogel by mixing HPC (a heat-responsive polymer), CTO (a photothermal material), and CNT (a heat-dissipation material) to produce a CCH thermoresponsive display. HPC changes its hydrophilic (coil)–hydrophobic (global) characteristics at temperatures above or below the LCST and can produce visible images through scattering by the aggregated global structure. When the NIR laser was irradiated locally only to the desired area, the CTO effectively absorbed and generated heat (photothermal effect) from the NIR, promoting the heat-responsive behavior of the HPC. When the NIR laser irradiation was stopped, the display heated above the LCST was restored to its initial state by the rapid heat conduction and cooling of the CNT. The operation of this CCH thermoresponsive display showed apparent differences depending on the change in the CNT content. When the on/off time of the NIR laser at 0 wt% CNT was 10/7 s, the maximum temperature was 41.84 °C, the delay was 1.9 s, and the off time was 5.6 s.

Meanwhile, when the on/off time of the NIR laser at 0.075 wt% CNT was 10/10 s, the maximum temperature was 43.62 °C, the delay was 1.4 s, and the off time was 1.5 s, shortening the delay and off time even though the temperature was relatively increased. This study improved the display operation of the CTO–HPC composite hydrogel by optimizing the photothermal effect of CTO and the heat dissipation characteristics of CNT, and various images (figures, letters, and constellation images) were implemented on flat and curved displays. The NIR-writing CCH thermoresponsive display produced in this study visualizes invisible light sources. Therefore, it can be used in fields that require security, such as the military, or in advertising displays that need to be replaced by beam projectors because of the long light projection distance. It is expected to be used in fields that convey information to several people, such as learning boards.

Conflicts of interest

The authors declare no completing financial interests.

Acknowledgements

This work was supported by the National Research Foundation of Korea (NRF) grant funded by the Korea government (MSIT) (2019R1A2C2010614, 2020R1A5A1019131, 2021R1I1A1A01060148, 2022R1C1C1008806, and 2022R1A2C1091961).

References

1 A. Halperin, M. Kröger and F. M. Winnik, *Angew. Chem., Int. Ed.*, 2015, **54**, 15342–15367.
2 G. Pasparakis and C. Tsitsilianis, *Polymer*, 2020, **211**, 123146.
3 A. Bordat, T. Boissenot, J. Nicolas and N. Tsapis, *Adv. Drug Delivery Rev.*, 2019, **138**, 167–192.
4 K. Wang, Q. Liu, G. Lu, Y. Zhang, Y. Zhou, S. Chen, Q. Ma, G. Liu and Y. Zeng, *Macromolecules*, 2021, **54**, 3725–3734.
5 M. Concilio, V. P. Beyer and C. R. Becer, *Polym. Chem.*, 2022, **13**, 6423–6474.
6 A. S. Hoffman, *Adv. Drug Delivery Rev.*, 2013, **65**, 10–16.
7 A. C. Hunter and S. M. Moghimi, *Polym. Chem.*, 2017, **8**, 41–51.
8 L. Ionov, *Mater. Today*, 2014, **17**, 494–503.
9 H. Kim, K. Kim and S. J. Lee, *NPG Asia Mater.*, 2017, **9**, e445.
10 R. Williams and G. S. Mittal, *LWT–Food Sci. Technol.*, 1999, **32**, 440–445.
11 Y. Suzuki and Y. Makino, *J. Controlled Release*, 1999, **62**, 101–107.
12 E. Weißenborn and B. Braunschweig, *Soft Matter*, 2019, **15**, 2876–2883.
13 G. Liu, J. Xu and R. Li, *Mater. Des.*, 2020, **194**, 108955.
14 K. Adachi and T. Asahi, *J. Mater. Res.*, 2012, **27**, 965–970.
15 A. Tan, S. Y. Madani, J. Rajadas, G. Pastorin and A. M. Seifalian, *J. Nanobiotechnol.*, 2012, **10**, 34.
16 F. Zhou, X. Da, Z. Ou, B. Wu, D. Resasco and W. Chen, *J. Biomed. Opt.*, 2009, **14**, 021009.
17 Z. Han and A. Fina, *Prog. Polym. Sci.*, 2011, **36**, 914–944.
18 D.-K. Lee, J. Yoo, H. Kim, B.-H. Kang and S.-H. Park, *Materials*, 2022, **15**, 1356.
19 M. Fettaka, R. Issaadi, N. Moulai-Mostefa, I. Dez, D. L. Cerf and L. Picton, *J. Colloid Interface Sci.*, 2011, **357**, 372–378.
20 T. P. Lodge, A. L. Maxwell, J. R. Lott, P. W. Schmidt, J. W. McAllister, S. Morozova, F. S. Bates, Y. Li and R. L. Sammler, *Biomacromolecules*, 2018, **19**, 816–824.
21 S. A. Arvidson, J. R. Lott, J. W. McAllister, J. Zhang, F. S. Bates, T. P. Lodge, R. L. Sammler, Y. Li and M. Brackhagen, *Macromolecules*, 2013, **46**, 300–309.
22 M. Gosecki, H. Setälä, T. Virtanen and A. J. Ryan, *Carbohydr. Polym.*, 2021, **251**, 117015.
23 Y. Jing and P. Wu, *Cellulose*, 2013, **20**, 67–81.
24 P. Khuman, W. B. K. Singh, S. D. Devi and H. Naorem, *J. Macromol. Sci., Part A*, 2014, **51**, 924–930.
25 H. Takeda and K. Adachi, *J. Am. Ceram. Soc.*, 2007, **90**, 4059–4061.
26 J.-X. Liu, Y. Ando, X.-L. Dong, F. Shi, S. Yin, K. Adachi, T. Chonan, A. Tanaka and T. Sato, *J. Solid State Chem.*, 2010, **183**, 2456–2460.
27 J. X. Liu, X. J. Wang, F. Shi, Z. J. Peng, J. Y. Luo, Q. Xu and P. C. Du, *Adv. Mater. Res.*, 2012, **531**, 235–239.
28 Z. Zhao, S. Yin, C. Guo and T. Sato, *J. Nanosci. Nanotechnol.*, 2015, **15**, 7173–7176.
29 C.-J. Chen and D.-H. Chen, *Nanoscale Res. Lett.*, 2013, **8**, 57.